JOURNAL OF
EMERGING INVESTIGATORS

Article

Analysis of bending loss in single-mode optical fiber with low-cost setup

Lucas Guan[1], Lijie Guan[2]
[1] Pinewood School, Los Altos Hills, CA
[2] Western Digital, San Jose, CA

SUMMARY

Optical fibers are essential for global communications, but bending loss remains a key factor limiting performance. We investigated how bending radius, wavelength, and number of turns influenced signal attenuation in a commercial single-mode fiber. We hypothesized that, at a fixed radius and wavelength, bending loss would increase linearly with the number of turns, while loss per turn across different radii would increase exponentially, with higher wavelengths exacerbating optical losses. To test this, we coiled fiber samples at different radii and measured output power at 1310 nm and 1550 nm using an optical power meter. Our results showed that at a given radius and wavelength, total loss increased linearly with the number of turns, while loss per turn across radii followed an exponential dependence. In addition, output power at 1550 nm exhibited higher losses than at 1310 nm at the same bend radius, confirming the predicted wavelength sensitivity. To interpret these trends, we obtained an analytical expression by fitting experimental results that captured bending-loss dependence on bend radius and wavelength. Fitting our data to an exponential model provided parameters that were qualitatively consistent with theoretical predictions, though the experimental wavelength dependence was weaker than expected. Overall, our results demonstrated that bending loss follows an exponential dependence on radius and is wavelength-dependent, with experimental trends qualitatively matching theoretical predictions. These findings underscore the value of combining low-cost experiments with analytical modeling to study fundamental properties of optical fibers and may help inform fiber routing decisions, especially in areas where bending attenuation matters.

INTRODUCTION

The inception of utilizing light waves to transmit information dates to 1880, when Alexander Graham Bell invented the photophone. Sunlight was regulated by a moving diaphragm and then carried through around 200 meters of open air before reaching a receiver that used a selenium cell to detect the signal (1). The idea of guiding light over long distances evolved in the early 1960s with the vision of optical fibers as optical elements. In 1970, researchers at Corning developed the first optical fiber with signal losses below 20 dB per kilometer, resulting in under 1% signal loss over each kilometer of transmission (2). In the early 1970s, fibers were developed that could replace copper cables for transmitting information over hundreds to thousands of miles (3). Unlike electrical signals, fiber-optic systems use light energy to relay information through pliable, transparent fibers made of glass or plastic. These fibers are often around the thickness of a human hair. Modern communication systems often favor optical fibers for long-range, high-data transmission because of their extremely low attenuation, which allows light to propagate with minimal power loss (4).

Despite these advantages, optical fibers are not free from transmission impairments. Loss mechanisms such as scattering, absorption, and bending losses can limit system performance. Among these, bending loss is particularly important because fibers in practical use are often coiled, routed around corners, or integrated into compact photonic devices (5). When an optical fiber is bent, part of the guided optical mode leaks into the cladding and radiates away, reducing the transmitted signal. This effect becomes stronger at smaller bending radii and longer operating wavelengths (5).

Theoretical descriptions of bending loss have been developed since the early work of Marcuse and others, which provided an analytical framework to estimate attenuation based on fiber parameters and bending geometry (6, 7). Specifically, the transmitted power P at propagation distance L is related to the input power P_0 by:

$$P = P_0 e^{-2\alpha L} \quad \text{(Equation 1)}$$

Here 2α is the power loss coefficient, with units of m^{-1}, and describes the rate at which optical power decays exponentially along the fiber due to bending. The Marcuse model provides an analytical expression for 2α:

$$2\alpha = \frac{\pi^{1/2}\kappa^2 \exp\left(-\frac{2\gamma^3 R}{3\beta^2}\right)}{2R^{1/2}\gamma^{3/2}V^2 K_{m-1}(\gamma a)K_{m+1}(\gamma a)} \quad \text{(Equation 2)}$$

where R is bending radius, a is the core radius, β is the propagation constant of the straight fiber, K_m are modified Bessel functions, κ and γ are the field decay rates in the core and cladding, respectively, with the following:

$$\kappa = (n_1^2 k^2 - \beta^2)^{\frac{1}{2}} \quad \text{(Equation 3)}$$

$$\gamma = (\beta^2 - n_2^2 k^2)^{1/2} \quad \text{(Equation 4)}$$

$$V = ka(n_1^2 - n_2^2)^{1/2} \quad \text{(Equation 5)}$$

κ and γ describe how quickly the optical field falls off away from the fiber axis and therefore how tightly light is confined. V is the normalized frequency, which characterizes how many modes the fiber can support. Equations 3-5 define each of these in terms of the core and cladding refractive indices, n_1 and n_2, respectively, and the wavenumber $k = 2\pi/\lambda$.

While Equation 2 provides a complete analytical

JOURNAL OF
EMERGING INVESTIGATORS
https://doi.org/10.59720/26-011

expression for *2α*, its complexity makes it difficult to use directly for experimental comparison. The dominant behavior is controlled by the exponential term in the numerator, which varies far more rapidly with *R* than any of the prefactor terms. In particular, the $R^{1/2}$ dependence appearing in the denominator of Equation 2 changes slowly compared to the exponential and is therefore absorbed into the overall scaling coefficient in the simplified model. The essential radius and wavelength dependence of bending loss can thus be simplified into a more practical form:

$$\alpha \propto A(\lambda)e^{-B(\lambda)R} \qquad \text{(Equation 6)}$$

where *A*(λ) and *B*(λ) are functions of wavelength λ.

In practical environments, fiber performance can deviate from theoretical predictions due to manufacturing tolerances, coating effects, and environmental conditions, so experimental characterization remains essential. In this work, we used a low-cost setup to measure bending loss of a commercial single-mode jumper and compared results to Equation 6 derived from Equation 2. We investigated bending-radius dependence, scaling with turn count (loss/turn), wavelength dependence, and agreement between fitted *A* and *B* and theoretical predictions.

We selected 1310 nm and 1550 nm as our test wavelengths because they are the two dominant wavelengths used in modern fiber-optic telecommunications. The ITU-T G.652 standard, which governs single-mode optical fiber specifications, designates these two wavelengths as the primary operating regions; 1310 nm is standard for short- to medium-range networks where bend constraints are tight, while 1550 nm is preferred for long-haul transmission due to its lower attenuation in silica fiber (8). These two wavelengths have also been tested in prior bending loss studies, making our results directly comparable to established theoretical and experimental predictions (7).

We hypothesized that bending loss would increase linearly with turn count at a fixed radius, increase exponentially with decreasing *R*, and be higher at longer wavelengths. We tested these predictions at 1310 nm and 1550 nm by measuring attenuation versus turns at fixed *R*, then fitting *A* and *B* at each wavelength. Our results supported both hypotheses: loss increased linearly with turn count at a fixed radius, and loss per turn scaled exponentially with decreasing radius. Additionally, 1550 nm consistently exhibited higher losses than 1310 nm at the same bend radius, supporting the predicted wavelength sensitivity. These results demonstrate that core bending-loss behavior can be captured with accessible instrumentation, with direct relevance to compact fiber-optic system design and broader implications for low-cost photonic education and research.

RESULTS

To test our hypotheses that bending loss increases linearly with turn count at a fixed radius, exponentially with decreasing bend radius, and is greater at longer wavelengths, we measured optical power attenuation in SMF-28 single-mode fiber at 1310 nm and 1550 nm across a range of bend radii and turn counts. The following results are organized to address each of these dependencies in turn.

Measurements and Units

We recorded all optical power measurements in decibel-milliwatts (dBm), a logarithmic unit expressing absolute optical power relative to 1 milliwatt, defined as *P*(dBm) = $10\log_{10}(P/1\text{mW})$. To quantify how bending radius, wavelength, and number of turns affected optical power loss, we coiled a commercial single-mode fiber around mandrels of different radii and measured the transmitted optical power (dBm) at both λ =1310 and 1550 nm, from which attenuation was derived by comparing output power to the baseline measurement taken at zero turns. To overcome the power meter's resolution (0.02 dBm) and improve accuracy, we increased the number of turns until the accumulated power loss exceeded the detection threshold. Each data point represents the average of three repeated measurements taken under near-identical conditions.

Loss per Turn

We first plotted transmitted power as a function of the number of coils wrapped around mandrels of various radii for λ =1550 nm (**Figure 1**). Next, we plotted the same measurements for λ =1310 nm (**Figure 2**). Across all tested radii, optical loss per turn increased linearly with the number of turns, with regression fits yielding R^2>0.95 in every case (**Figure 1 and Figure 2**). This suggested that, once the bend radius and wavelength were fixed, each additional loop contributed linearly to total attenuation. Therefore, the slope of the best-fit line represented loss per turn. The loss per turn was observed at both wavelengths, and the loss per turn values differed substantially between wavelengths. For example, at a 10.9 mm bend radius, the λ =1550 nm measurements showed a slope of ~0.028 dBm/turn, while at λ =1310 nm the slope was about an order of magnitude smaller (~0.004 dBm/turn).

Loss per Turn vs. Radius

Loss per turn values were plotted as a function of bend

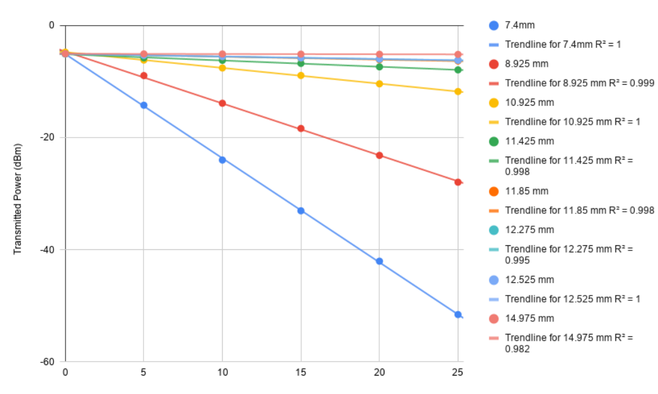

Figure 1: Transmitted power (dBm) versus number of turns for various bend radii at 1550 nm. Line graph showing transmitted optical power (dBm) as a function of turn count for SMF-28 single-mode fiber coiled at bend radii ranging from 7.4 mm to 14.975 mm. Measurements were taken at 1550 nm using an ORIENTEK TLT-12E optical power meter and light source. Each data point represents the mean of three replicate trials (*n* = 3). Goodness-of-fit was quantified using the coefficient of determination (R^2 > 0.98). Linear regression slopes were used to calculate average loss per turn.

radius, revealing how attenuation scaled with bending geometry across both wavelengths (**Figure 3**). The dependence appeared nonlinear, suggesting an exponential relationship. To test this, the data were replotted on a semi-logarithmic scale, where loss per turn was plotted against bend radius with a logarithmic y-axis (**Figure 4**). The close alignment of both datasets with straight lines suggested an exponential relationship of the form:

$$\alpha(R) = Ae^{-BR} \quad \text{(Equation 7)}$$

where *α* is loss per turn (dBm/turn), *A* is a scaling constant, *B* is the exponential decay constant controlling how steeply loss decreases with radius, and *R* is the bend radius. To extract *A* and *B*, Equation 7 was log-linearized into:

$$\ln(\alpha) = \ln(A) - BR \quad \text{(Equation 8)}$$

yielding straight-line fits with slope −*B* and intercept ln(*A*) (**Figure 4**). At λ = 1550 nm, the best-fit parameters were *A* = 968.0, *B* = 0.800 mm^{-1}. At λ = 1310 nm, the fit yielded *A* = 192.9, *B* = 1.026 mm^{-1}. Because 1550 nm data had more points, the trend line for that graph was clearer compared to that of the 1310 nm data, where only 3 data points could be measured due to larger radii producing losses below the optical power meter's sensitivity.

Wavelength Dependence

Looking at the fitting results, at a given bend radius, bending loss seemed to increase with wavelength. Comparing parameters, *A* set the overall loss scale, with higher values indicating greater sensitivity to bending. *B* set the steepness of the exponential decay, with larger values meaning loss falls off faster with radius. Since the exponential term dominates, we focused on analysis of *B*(λ). To gain a quantitative understanding of wavelength dependence of the *B* value, we compared our experimental results with theoretical predictions. From Equation 2, *B*(λ) roughly scales with γ^3. From Equation 4, γ roughly scales with λ^{-1}. Therefore,

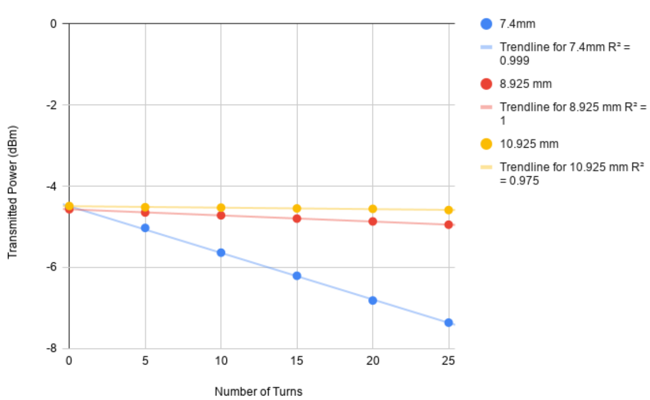

Figure 2: Transmitted power (dBm) versus number of turns for various bend radii at 1310 nm. Line graph showing transmitted optical power (dBm) as a function of turn count for SMF-28 single-mode fiber coiled at bend radii of 7.4 mm, 8.925 mm, and 10.925 mm. Measurements were taken at 1310 nm using an ORIENTEK TLT-12E optical power meter and light source. Each data point represents the mean of three replicate trials (*n* = 3). Goodness-of-fit was quantified using the coefficient of determination ($R^2 > 0.97$). Linear regression slopes were used to calculate average loss per turn.

B(λ) should roughly scale with λ^{-3}. The ratio *B*(1310)/ *B*(1550) should be $(1310/1550)^{-3}$ =1.65, based on theoretical scaling. Loss per turn values at λ =1550 nm were higher than those at λ =1310 nm, consistent with the higher *A* value at λ =1550 nm (**Figure 4**). However, the slope of the linear fit (corresponding to -*B*) was lower at λ =1550 nm than at λ =1310 nm, meaning that loss per turn was more sensitive to radius at λ =1310 nm. Our experimental ratio *B*(1310)/*B*(1550) = 1.28, which is within the same order of magnitude as the theoretical prediction of 1.65.

DISCUSSION

Our results suggest three dependencies of bending loss in single-mode fibers: linear increase with the number of turns at a fixed radius and wavelength, exponential increase with decreasing bend radius, and increased loss at longer wavelengths.

Specifically, both the theoretical and experimental ratios for the *B* value exceed 1.0, supporting the key qualitative prediction: *B* is larger at shorter wavelengths, meaning that loss per turn falls off more steeply with radius at 1310 nm than at 1550 nm. Physically, this makes sense because longer wavelengths are harder to confine within the narrow fiber core. At longer wavelengths, more of the light energy already extends into the surrounding cladding region even before any bending occurs, making it easier for a bend to cause that energy to radiate away. At shorter wavelengths, light is more tightly concentrated in the core, so a sharper bend is needed before significant leakage begins, and once that threshold is crossed, loss rises steeply with decreasing radius, producing the larger *B* value observed at 1310 nm. Quantitatively, our results were lower than the theoretical value, which could reflect both limited experimental sampling and the possibility that the underlying model is too simplistic, since it assumes idealized fiber geometry and ignores factors such as optical mode-field distribution and fiber manufacturing variations. This suggests that while the theoretical model captures the overall scaling behavior, more sophisticated treatments are needed for precise quantitative predictions. For example, Schermer and Cole developed an improved bend loss formula that accounts for the full mode-field distribution and transition loss at the onset of the bend (7). Numerical approaches such as finite-element or beam-propagation simulations could similarly capture fiber geometry and coating effects that the simplified model ignores.

These results highlighted two important points. First, the exponential dependence of loss per turn on bend radius was consistent across both wavelengths and all tested radii. Second, the wavelength dependence observed here is physically meaningful even with limited 1310 nm data and reflects the fundamental scaling of bending loss in single-mode fibers. From an applications perspective, this explains why 1310 nm transmission is often used in local-area networks with tight bend constraints, while 1550 nm is more common in long-haul systems where bends can be minimized and low attenuation is critical.

Three major limitations should be considered when interpreting our data. First, only two wavelengths were tested due to equipment restrictions, preventing exploration of a broader wavelength range and more precise dependency.

https://doi.org/10.59720/26-011

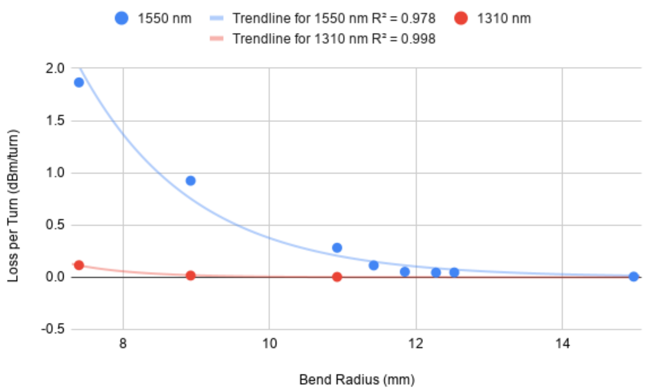

Figure 3: Loss per turn vs. bend radius at 1310 nm and 1550 nm. Scatter plot showing average loss per turn (dBm/turn) for SMF-28 single-mode fiber coiled at bend radii ranging from 7.4 mm to 14.975 mm. Loss per turn values were derived from the slopes of linear regressions of transmitted power versus turn count. Data sets for 1310 nm and 1550 nm were independently fitted with the exponential model in Equation 4. Goodness-of-fit was quantified using the coefficient of determination ($R^2 > 0.97$). Each slope was calculated from a single measurement series ($n = 1$).

Second, the accuracy of the 1310 nm radius dependence was limited: only three radii were measured. At very small radii (<7.4 mm), fiber degradation or mechanical strain occurred, while at large radii (>15 mm), losses were below our detection threshold despite increasing turn count. Third, repeated use of the same fiber and instruments may have introduced degradation effects, influencing accuracy. Despite these limitations, the consistency of the linear and exponential trends across conditions strongly supported the robustness of our conclusions.

Future studies should expand the range of wavelengths tested to provide a more comprehensive understanding of how bending loss scales across the optical spectrum. In particular, testing shorter wavelengths (<1000 nm) could corroborate the stronger confinement predicted by theory, while testing longer wavelengths (>1600 nm) would provide insight into regimes where loss becomes more severe. Improved measurement accuracy, such as using a higher-resolution optical power meter and repeating trials with multiple fiber samples, would help reduce uncertainty and increase statistical reliability. Additional experiments could also investigate the effects of fiber type, such as bend-insensitive fibers, to determine how structural modifications mitigate loss compared to standard SMF-28.

In summary, this study demonstrated that bending loss in single-mode optical fiber follows predictable and theoretically grounded trends across bend radius, turn count, and wavelength. Loss increased linearly with turn count at a fixed radius, exponentially with decreasing bend radius, and was consistently higher at 1550 nm than at 1310 nm; these are all consistent with predictions derived from the Marcuse model. While quantitative agreement with theory was restricted by experimental constraints and model limitations, the qualitative scaling behavior was consistently observed. Beyond the specific findings, this work demonstrates that fundamental fiber-optic phenomena can be meaningfully investigated using low-cost, commercially available equipment, without the need for specialized laboratory infrastructure. This has practical implications for compact fiber-optic network design, where understanding bending loss is critical for routing fibers in tight spaces, and broader implications for making fiber-optic experimentation accessible in educational and resource-limited research settings.

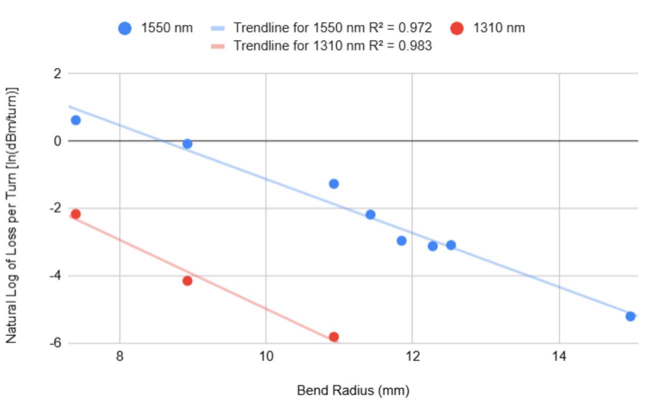

Figure 4: Semi-logarithmic plot of loss per turn versus bend radius at 1310 nm and 1550 nm. Scatter plot showing the natural logarithm of loss per turn ln(dBm/turn) as a function of bend radius (mm) for SMF-28 single-mode fiber at 1310 nm and 1550 nm. Linear regression analysis was performed in Google Sheets, and goodness-of-fit was assessed by the coefficient of determination ($R^2 > 0.97$). Each slope was derived from a single measurement series ($n = 1$).

MATERIALS AND METHODS

Fiber and Optical Measurement Equipment

The experiments were conducted using a 10 m single-mode fiber optic jumper cable (SMF-28, Subscriber Connectors (SC)-SC connectors, Amazon). SMF-28 is a standard single-mode fiber commonly used in telecommunications, with a mode field diameter of approximately 9 µm at 1310 nm and 10.4 µm at 1550 nm, and a cladding diameter of 125 µm. The cable was jacketed, pre-terminated with SC connectors, and did not require cleaving or splicing during testing. Optical signals were provided by the ORIENTEK TLT-12E FTTH Tool Kit (Amazon), which includes a dual-wavelength optical light source (OLS) at 1310 nm and 1550 nm, an optical power meter (OPM), and a visible fault locator. The OLS produces a stable continuous-wave output, and the OPM records transmitted power in dBm units with a resolution of 0.02 dBm. This instrument set was chosen to balance affordability with sufficient accuracy for detecting small attenuation changes associated with bending loss.

Bend Radius Setup

To generate repeatable bend radii, the fiber was coiled around cylindrical mandrels of different diameters. A variety of household objects were used as mandrels, each measured with digital calipers to determine precise diameters. The objects included a PVC pipe (27.0 mm diameter), mop handle (22.1 mm), wooden dowel (18.9 mm), drumstick (14.9 mm), and the handle of a broom (11.85 mm). To expand the available range of radii, sheets of A4 printer paper were wrapped around the wooden dowel in layers, producing effective diameters of 19.9 mm, 20.75 mm, and 21.6 mm.

Because the fiber optic cable itself had an outer jacket

https://doi.org/10.59720/26-011

diameter of 2.95 mm, the effective bend radius was not simply half the object diameter. Instead, the bending radius was measured from the center of the mandrel to the center of the fiber core, requiring an additional 1.475 mm (half the cable diameter) to be added. The effective bend radius was therefore calculated as:

$$D_{eff} = \frac{D_{object}}{2} + \frac{D_{fiber}}{2} \quad \text{(Equation 9)}$$

where D_{object} is the mandrel diameter and D_{fiber} the 2.95 mm fiber cable diameter. For example, the 18.9 mm wooden dowel produced an effective radius of 10.925 mm rather than 9.45 mm. Using this method, the tested bend radii spanned from 7.4 mm to 14.975 mm. All values were confirmed with calipers to within ±0.05 mm.

Preliminary attempts to coil the fiber around smaller mandrels, such as pencils with radii below 7.4 mm, consistently resulted in fiber damage. This was evident because repeated trials gave abnormally high and extremely variable loss values, indicating that the fiber core had fractured. Based on these observations, the broom handle (7.4 mm effective radius) was identified as the smallest radius at which the fiber could be bent without permanent damage. This constraint established the lower bound of radii tested in this study.

Experimental Setup and Procedure

Before each trial, the fiber connectors were cleaned using lint-free optical wipes and isopropyl alcohol to minimize insertion loss. The fiber was then connected between the OLS and OPM with SC connectors, and both devices were taped securely to a flat table to reduce motion and coupling variability. A short segment of the fiber near the connectors was also taped to the table to prevent strain or shifting during coiling. For each radius, the fiber was coiled around the mandrel in increments of five turns, starting from zero and increasing to a maximum of twenty-five turns. Care was taken to ensure that the fiber was wrapped evenly and without kinks, with each coil placed tightly against the previous one. Output power was recorded at each increment of turns. This process was repeated for all mandrels at both 1310 nm and 1550 nm wavelengths. However, measurable attenuation at 1310 nm was only observed for the three smallest radii (10.925 mm, 8.925 mm, and 7.4 mm), as larger radii produced losses below the instrument's sensitivity. Each measurement was taken three times and the data analyzed represents the average of the three trials.

Data Analysis

For each radius and wavelength, transmitted power was recorded at zero turns (baseline) and at increasing numbers of turns. To quantify attenuation, transmitted power (dBm) was plotted against turn count, and linear regression was applied. The slope of the fit, expressed in negative dBm per turn, was taken as the average loss per turn. This supported the expected linear scaling of attenuation with additional loops. To examine the dependence on bend radius, average loss per turn was plotted against radius, and an exponential model, Equation 4 was fitted independently to the 1310 nm and 1550 nm data sets. Model performance was assessed using the coefficient of determination (R^2). All data recording, plotting, and regression calculations were performed in Google Sheets.

Received: January 11, 2026
Accepted: April 30, 2026
Published: August 3, 2026

REFERENCES

1. Hecht, Jeff, "The Quest for Remote Viewing", *City of Light: The Story of Fiber Optics*. 2nd ed., Oxford University Press, 1999, pp. 34-45.
2. Li, Ming-Jun, and Nolan, Daniel A., "*Optical Transmission Fiber Design Evolution*", Journal of Lightwave Technology, vol. 26, no. 9, 2008, pp. 1079-1092. https://doi.org/10.1109/JLT.2008.922150
3. Bailey, David, and Wright, Edwin, "Historical Background to Fiber Optics", *Practical Fiber Optics*, 1st ed., Newnes (an Elsevier imprint), 2003, pp. 2-4.
4. Dutton, Harry J. R., "Optical Fibre", *Understanding Optical Communications*, 1st ed., Prentice Hall, 1998. pp. 25-33.
5. Allard, Frederick C., "Optical Fibers", *Fiber Optics Handbook for Engineers and Scientists,* McGraw-Hill, 1990, pp. 39-58.
6. Marcuse, Dietrich, "*Curvature Loss Formula for Optical Fibers*", Journal of the Optical Society of America, vol 66, no. 3, 1976, pp. 216-220. https://doi.org/10.1364/JOSA.66.000216
7. Schermer, Ross, and Cole, James, "*Improved Bend Loss Formula Verified for Optical Fiber by Simulation and Experiment*", IEEE Journal of Quantum Electronics, vol. 43, no. 10, 2007, pp. 899–909. https://doi.org/10.1109/JQE.2007.903364
8. International Telecommunication Union, "Characteristics of a Single-Mode Optical Fibre and Cable", ITU-T Recommendation G.652, 2024.